JVI Journals.ASM.org

Internal Ribosome Entry Site-Based Attenuation of a Flavivirus Candidate Vaccine and Evaluation of the Effect of Beta Interferon Coexpression on Vaccine Properties

Michael Frese,[a,b] Eva Lee,[b] Maximilian Larena,[a]* Pek Siew Lim,[b] Sudha Rao,[b] Klaus I. Matthaei,[a] Alexander Khromykh,[c] Ian Ramshaw,[a,b] Mario Lobigs[c]

John Curtin School of Medical Research, The Australian National University, Canberra, ACT, Australia[a]; Faculty of Education, Science, Technology and Mathematics, University of Canberra, Canberra, ACT, Australia[b]; Australian Infectious Diseases Research Centre, School of Chemistry and Molecular Biosciences, The University of Queensland, St Lucia, QLD, Australia[c]

ABSTRACT

Infectious clone technologies allow the rational design of live attenuated viral vaccines with the possibility of vaccine-driven coexpression of immunomodulatory molecules for additional vaccine safety and efficacy. The latter could lead to novel strategies for vaccine protection against infectious diseases where traditional approaches have failed. Here we show for the flavivirus *Murray Valley encephalitis virus* (MVEV) that incorporation of the internal ribosome entry site (IRES) of *Encephalomyocarditis virus* between the capsid and prM genes strongly attenuated virulence and that the resulting bicistronic virus was both genetically stable and potently immunogenic. Furthermore, the novel bicistronic genome organization facilitated the generation of a recombinant virus carrying an beta interferon (IFN-β) gene. Given the importance of IFNs in limiting virus dissemination and in efficient induction of memory B and T cell antiviral immunity, we hypothesized that coexpression of the cytokine with the live vaccine might further increase virulence attenuation without loss of immunogenicity. We found that bicistronic mouse IFN-β coexpressing MVEV yielded high virus and IFN titers in cultured cells that do not respond to the coexpressed IFN. However, in IFN response-sufficient cell cultures and mice, the virus produced a self-limiting infection. Nevertheless, the attenuated virus triggered robust innate and adaptive immune responses evidenced by the induced expression of Mx proteins (used as a sensitive biomarker for measuring the type I IFN response) and the generation of neutralizing antibodies, respectively.

IMPORTANCE

The family *Flaviviridae* includes a number of important human pathogens, such as *Dengue virus*, *Yellow fever virus*, *Japanese encephalitis virus*, *West Nile virus*, and *Hepatitis C virus*. Flaviviruses infect large numbers of individuals on all continents. For example, as many as 100 million people are infected annually with *Dengue virus*, and 150 million people suffer a chronic infection with *Hepatitis C virus*. However, protective vaccines against dengue and hepatitis C are still missing, and improved vaccines against other flaviviral diseases are needed. The present study investigated the effects of a redesigned flaviviral genome and the coexpression of an antiviral protein (interferon) on virus replication, pathogenicity, and immunogenicity. Our findings may aid in the rational design of a new class of well-tolerated and safe vaccines.

The well-established methodologies for generation of infectious cDNA clones have enabled the rational design of live viral vaccines using strategies beyond the simple incorporation into the viral genome of a series of attenuation markers that are the basis for the reduced pathogenicity of traditional live vaccines. A recent example is the concept of "codon pair deoptimization" tested for experimental vaccines against *Poliovirus* (1) and *Influenza A virus* (2). Targeted insertion into these viruses of hundreds of point mutations that change codon usage without changing protein sequence greatly reduced the virulence but not the immunogenicity of live vaccine candidates. A second example of a rational attenuation strategy that targets the level and balance of protein production without altering protein sequence is that of internal ribosome entry site (IRES)-based attenuation developed for the alphaviruses *Chikungunya virus* (3) and *Venezuelan equine encephalitis virus* (4–6). It involved replacement of the alphaviral subgenomic promoter with an IRES of *Encephalomyocarditis virus* (EMCV). Preclinical trials showed protective immunity with IRES-based alphavirus vaccine candidates despite their highly attenuated virulence phenotypes. The strategy also prevented viral replication in mosquito vectors, thereby eliminating the risk of natural transmission of these recombinant arboviruses.

Here we have employed an IRES-based attenuation strategy to produce a flavivirus vaccine candidate. The family *Flaviviridae* includes a number of important human pathogens such as *Dengue virus*, *Yellow fever virus*, *Japanese encephalitis virus*, *West Nile virus*, and *Hepatitis C virus*. New or improved vaccines are urgently needed against several flaviviral diseases, most notably dengue and hepatitis C. Viruses belonging to the *Flaviviridae* have a plus-strand RNA genome that is translated into a single polyprotein that is subsequently cleaved by host and viral proteases into the

Received 29 October 2013 **Accepted** 27 November 2013
Published ahead of print 4 December 2013
Address correspondence to Mario Lobigs, m.lobigs@uq.edu.au.
* Present address: Maximilian Larena, Institute of Biomedicine, The Sahlgrenska Academy, University of Gothenburg, Gothenburg, Sweden.

doi:10.1128/JVI.03051-13

mature viral proteins. IRES-based attenuation of a flavivirus would alter its monocistronic genome organization and generate a bicistronic genome that would preclude an equimolar production of viral proteins from a single precursor, unless the IRES were introduced into the 3′ untranslated region (UTR). A bicistronic flavivirus genome organization would also offer the possibility of fine-tuning the immune and safety properties of a vaccine candidate by introducing genes for immunomodulatory molecules such as interferon (IFN) or other cytokine genes.

IFNs were discovered over 50 years ago as the most potent antiviral factors of the innate immune system (reviewed in reference 7). The human genome encodes 16 different type I IFNs, i.e., 12 IFN-α subtypes plus IFN-β, -ε, -κ, and -ω (8). Research has largely been focused on IFN-α and -β, which are secreted by most virus-infected cells and highly specialized leukocytes called natural IFN-producing cells or plasmacytoid dendritic cells (9). IFNs act by regulating the expression of a multitude of IFN-induced cellular factors, many of which inhibit viral replication (10). The direct antiviral activity of these factors slows down the spread of the infection, reduces the viral load, and in some cases can even eliminate the infection. In addition, type I IFNs act as critical factors linking innate and adaptive immunity (reviewed in reference 11). For example, they promote the differentiation, maturation, and migration of dendritic cells and potently enhance humoral and cellular immunity. A deeper understanding of the IFN system has led to therapeutic application of IFNs not only for viral diseases but also for cancer and multiple sclerosis and has underscored the potential for an expansion of their clinical application, for example, as immunological vaccine adjuvants (reviewed in reference 12). IFN coexpression with a recombinant live vaccine is hence predicted to not only stimulate the local innate antiviral immune system, but also provide an adjuvant effect by promoting local humoral and cellular immune responses in antigen-draining lymph nodes. Viral coexpression of IFN can therefore boost the immunogenicity and therapeutic potential of replication-competent viral vectors, while reducing their ability to spread and cause disease (see, for example, references 13 to 17).

In this study, we have produced the first IRES-based attenuated flavivirus candidate vaccine and the first flavivirus encoding an IFN. *Murray Valley encephalitis virus* (MVEV) was chosen as a model flavivirus, because well-characterized mouse models that mimic the virulence and pathogenesis observed in humans are available (reviewed in reference 18), and immune responses important in recovery from primary infection and in vaccine protection against neurotropic flaviviruses have been defined (reviewed in reference 19). Furthermore, we address questions relating to the effect of bicistronic genome organization and IFN-β coexpression on vaccine safety and efficacy.

MATERIALS AND METHODS

Mice. C57BL/6 (B6), BALB/c, IFN-α/β receptor knockout (IFNAR$^{-/-}$) (20), NOD-*scid* (21), and BALB.A2G-*Mx1* mice were bred under specific-pathogen-free conditions and supplied by the Animal Breeding Facility at the John Curtin School of Medical Research, The Australian National University, Canberra. Congenic BALB.A2G-*Mx1* mice were generated locally by crossing B6.A2G-*Mx1* with Mx1-negative BALB/c mice (10 backcrosses after the initial cross). Six- to 8-week-old mice were used in virulence and vaccination experiments, unless indicated otherwise. Mice were infected intraperitoneally (i.p.), intravenously (i.v.), subcutaneously (s.c.), or intramuscularly (i.m.) with a defined virus dose in 0.1 ml of Hanks' balanced salt solution (HBSS) containing 20 mM HEPES (pH 8.0) and 0.2% bovine serum albumin (HBSS-BSA). For intracranial (i.c.) infections, 3- to 4-week-old weanling mice were anesthetized with 50 μl of a 10% ketamine-xylazole solution in phosphate-buffered saline (PBS) by i.p. injection, and a defined dose of virus diluted in 20 μl HBSS-BSA was inoculated into the right hemisphere of the brain. Mice were monitored twice daily, and severely moribund mice were euthanized by cervical dislocation.

Cells and viruses. African green monkey kidney (Vero) cells were obtained from the American Type Culture Collection and grown in Eagle's minimal essential medium (EMEM) plus nonessential amino acids and 5% fetal bovine serum (FBS). Mouse embryo fibroblasts (MEFs) were established from B6 or IFNAR$^{-/-}$ mice and maintained in EMEM plus nonessential amino acids and 10% FBS. An infectious MVEV clone derived from the prototype strain MVEV-1-51 (22) was used for the generation of bicistronic MVEV constructs (see below) and to produce working stocks of wild-type (wt) virus. All virus stocks, including those containing the newly generated viruses, MVEV.IFN-β and MVEV.C-IRES (see below), were generated by standard procedures (22). Briefly, plasmid DNA was linearized with NsiI, and infectious full-length RNA was synthesized *in vitro* using T7 RNA polymerase and electroporated into BHK cells that were cultured for 3 to 4 days to allow the accumulation of virus in the culture supernatant. Following an additional passage in Vero cells, virus stocks were stored in single-use aliquots at −80°C and titrated by plaque assay on Vero cells, as previously described (23).

Construction of bicistronic viruses. A 2,574-bp ApaI/XbaI fragment encompassing the 5′ 1,943 bp of the MVEV infectious clone plasmid pM212 (22) plus an amber termination codon at the 3′ end of the C gene followed by the EMCV IRES (version as present in pCITE-2a; for example, see reference 24) was excised from a eukaryotic expression plasmid used to construct the replicon packaging cell line 293.C.IRES-prM-E (25) and subcloned into pMVEV-FL-v2 (25) digested with the same enzymes. The derivative plasmid (pMVEV-FL-C.IRES) was modified by removing an NsiI restriction site present in the IRES cDNA.

The mouse IFN-β gene (GenBank accession number NM_010510.1) was inserted into plasmid pMVEV-FL-C.IRES as a 1,098-bp ApaI fragment excised from a synthetically synthesized DNA product (GenScript, Piscataway, NJ). The IFN-β gene, lacking its own signal peptide sequence, was positioned immediately downstream of the MVEV prM signal sequence, allowing translocation of the IFN into the lumen of the endoplasmic reticulum (ER) and subsequent secretion. Cap-dependent translation of viral capsid and IFN-β proteins was terminated at the authentic C-terminal amino acid of the IFN protein sequence. The introduction of the downstream EMCV IRES drives translation of the remaining viral polyprotein starting with the prM sequence. The prM signal peptide sequence upstream of the IRES was modified by synonymous mutations (details are given in Fig. 1) to prevent homologous recombination between it and the authentic downstream prM signal peptide.

Quantitation of IFN-β protein synthesis. The IFN-β concentration in infected Vero cell culture supernatants was measured using an enzyme-linked immunosorbent assay (ELISA) kit specific for mouse IFN-β (PBL InterferonSource, Piscataway, NJ) following the manufacturer's recommended protocol.

Quantitative reverse transcription-PCR (RT-PCR). Total RNA was extracted from snap-frozen brain tissue samples using Tri Reagent (Molecular Research Center, Cincinnati, OH). The concentration of MVEV genomic RNA was determined essentially as previously described (25). Briefly, RNA was reverse transcribed, and quantitative real-time PCR was performed using the primers 5′-AACTCCAAGAATCTGGCTCCCA-3′ (downstream) and 5′-GGAAATGGTGGATGAGGAAAGG-3′ (upstream). Each RNA sample was tested in duplicate, and genome equivalent (GE) concentrations were determined by extrapolation from a standard curve generated within each experiment. *In vitro*-transcribed MVEV RNA was used as a standard. The detection limit of the assay was ~10^5 GEs/ml.

For IFN-α and Mx1 mRNA quantification, RNA (5 μg) was reverse

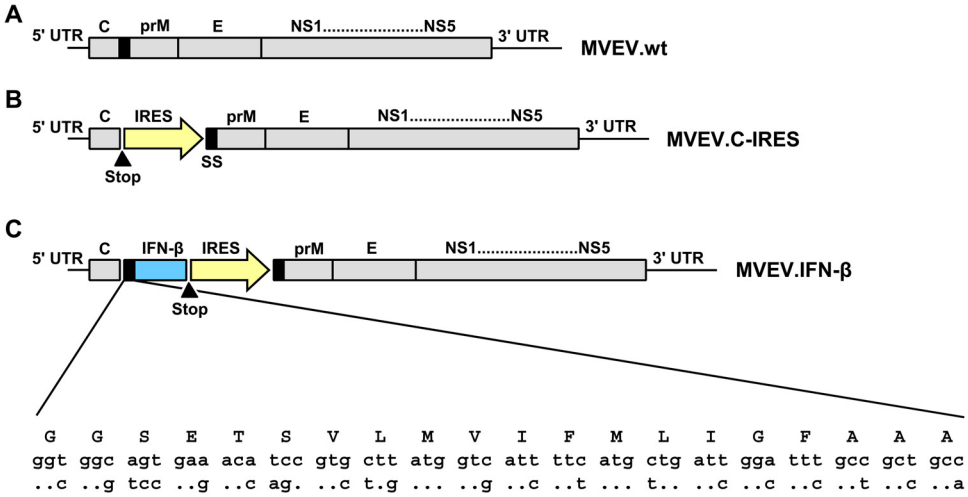

FIG 1 Schematic representation of the wild-type MVEV genome and two genetically engineered, bicistronic MVEV-based constructs. (A) MVEV.wt has a single, long open reading frame encoding all structural (C, prM, and E) and nonstructural (NS1 to NS5) proteins and flanked by untranslated regions (5′ and 3′ UTR). (B) For construction of MVEV.C-IRES, an opal stop codon (filled triangle) was introduced at the C terminus of C protein, followed by an EMCV IRES, which drives translation of all other viral proteins, starting at the signal peptide of prM (black box). (C) Construct MVEV.IFN-β has the mouse IFN-β gene (blue box) inserted downstream of the prM signal peptide, which directs the nascent IFN protein into the lumen of the ER; the IFN-β gene is flanked at the 3′ end by an opal stop codon (filled triangle), followed by EMCV IRES sequence (yellow arrow). The amino acid sequence (single-letter code) and corresponding nucleotide sequence of the prM signal peptide are shown at the bottom (60). Note that synonymous nucleotide changes were introduced into the prM signal peptide upstream of the IRES in construct MVEV.IFN-β to prevent homologous recombination and deletion of the foreign sequences from the viral genome (see sequence alignment; the top and bottom nucleotide sequences encode the wild-type and the altered prM signal peptide, respectively; the resulting amino acid sequence is in uppercase letters, and dots represent identical residues).

transcribed with the Maxima first-strand cDNA synthesis kit (Thermo Fisher Scientific, Waltham, MA). Quantitative real-time PCR was performed using the TaqMan gene expression assay in a total volume of 10 μl with a 1/100 cDNA dilution, according to the manufacturer's guidelines (Applied Biosystems, Foster City, CA). The following mouse TaqMan probes were used: *Mx1*, Mm00487796_m1; *IFN*-β, Mm00439552_s1; and *L32* (ribosomal protein L32), Mm02528467_g1 (Applied Biosystems). Each PCR was performed in duplicate. Threshold cycle values from the PCR amplification plots were converted to arbitrary copy numbers as described previously (26). The gene transcript levels were normalized to the housekeeping *L32* gene.

Serial passage and genetic stability of bicistronic MVEV. Infectious clone-derived MVEV.IFN-β and MVEV.C-IRES recovered from electroporated BHK cells were passaged 10 times in Vero cells. Briefly, cells were infected with a multiplicity of ~1, virus was grown for 3 to 4 days, and culture fluids were harvested when signs of cytopathic effects were apparent. To investigate the genome stability of bicistronic viruses by RT-PCR, Vero cells were infected with virus samples from the passage series at a multiplicity of ~1, and total RNA was extracted at 3 days postinfection (p.i.) using TRIzol reagent (Invitrogen/Life Technologies, Carlsbad, CA) and suspended in 20 μl of nuclease-free water. RNA was reverse transcribed using random hexamer primers (Promega, Fitchburg, WI), and PCR was performed as described previously (27) using an oligonucleotide primer pair (5′-GGAACACTGATTGATGTGGTGAAC-3′ [forward] and 5′-TGTGATCTGCCCGCTTCGTG-3′ [reverse]) that anneals to sequences in the C and E genes, respectively. The resulting amplicon spans the entire foreign gene insert, which allowed for the detection of major deletions in the IFN and/or IRES sequences and nucleotide sequencing of the IFN gene.

Serological test. For titration of MVEV-reactive antibodies in mouse serum, ELISAs were performed with horseradish peroxidase-conjugated goat anti-mouse Ig and the peroxidase substrate 2,2′-azino-di(3-ethylbenzthiasoline sulfonate), as described previously (28). For determination of ELISA endpoint titers, absorbance cutoff values were established as the mean absorbance in 8 negative-control wells containing sera of naive mice plus 3 standard deviations. Absorbance values of test sera were considered positive if they were equal to or greater than the absorbance cutoff, and endpoint titers were calculated as the log of the reciprocal of the last dilution giving a positive absorbance value. Neutralization titers measured in a 50% plaque reduction neutralization test ($PRNT_{50}$) were determined as previously described (29).

B cell transfer. B6 mice were sacrificed at 9 weeks after completion of a two-dose i.m. immunization schedule with 10^5 PFU of MVEV.C-IRES or MVEV.IFN-β, spleens aseptically removed, and single-cell suspensions prepared by pressing the spleen tissue gently through a fine metal mesh tissue sieve. Erythrocytes were lysed by suspending the splenocyte pellet in 4.5 ml distilled water, followed immediately by the addition of 0.5 ml of 10× PBS. Lysed cells were discarded after centrifugation at 400 × *g* for 5 min. For B cell enrichment, isolated splenocytes were incubated with 1:3 dilutions of anti-CD4 (RL172) plus anti-CD8 (31M) hybridoma supernatant in MEM plus 5% FBS for 30 min at 4°C, followed by incubation with rabbit serum complement (Cedarlane Laboratories, Burlington, Ontario, Canada) for 30 min at 37°C. Cells were washed twice with PBS before transfer into recipient mice. The efficiency of depletion of $CD4^+$ and $CD8^+$ cells was >95% as assessed by flow cytometry (data not shown). Immune or naive B cells (1×10^7 cells) were resuspended in 100 μl PBS and injected i.p. into 4-week-old B6 recipient mice. Recipient mice were challenged a day later with 1×10^5 PFU MVEV via footpad injection.

Immunohistochemistry and immunohistofluorescence analysis. After dissection, brain tissue samples were placed in 10% neutral buffered formalin fixative and stored at room temperature for at least 6 weeks before sagittal tissue sections of 4 μm in thickness were prepared and mounted on slides. For immunohistochemistry, sections were immunostained using the mouse monoclonal antibody M143 (directed against the human MxA protein; M143 recognizes a conserved epitope in the N-terminal region of Mx proteins and cross-reacts with murine Mx1 [30]), 4G4 (cross-reactive against the flavivirus NS1 protein [31]), and the LSAB2 system horseradish peroxidase (HRP) kit (Dako Denmark A/S, Glostrup, Denmark), essentially as described previously (32). Sections were then counterstained with either hematoxylin (in combination with 4G4) or

eosin (with M143). Slides were examined using an Olympus IX 71 microscope.

Statistical analyses. Standard deviations were calculated using Excel functions. Mortality data were plotted into Kaplan-Meier curves and assessed for significance by the log rank test.

Ethics statement. All animal experiments were approved by the Australian National University (ANU) Animal Ethics Committee (protocol number J.IG.76.09), under guidelines of the National Health and Medical Research Council of Australia (NHMRC).

RESULTS

Construction of bicistronic MVEV and viral coexpression of IFN-β. MVEV contains a relatively small genome of ~10.7 kb in length. Its only open reading frame is translated into a polyprotein that is proteolytically processed into at least 10 viral proteins (Fig. 1). To construct a vaccine candidate with IRES-based attenuation, a bicistronic virus (MVEV.C-IRES) was produced by inserting a termination codon followed by the EMCV IRES downstream of the coding sequence of the capsid (C) protein (Fig. 1). In this artificially generated genome, translation of the C protein occurs by a 5′-cap-dependent mechanism, while that of all other viral proteins (prM to NS5) is driven by the IRES, which reduces the likelihood of mutations that delete or damage the IRES.

For coexpression of an immunomodulatory cytokine with the bicistronic vaccine candidate, the mouse IFN-β-coding sequence followed by the EMCV IRES was inserted between the coding sequences for the C protein and the precursor-to-membrane (prM) protein (Fig. 1). In this construct (MVEV.IFN-β), the signal sequence for prM serves for ER luminal translocation of the IFN. To ascertain translocation of prM, a second copy of the prM signal peptide was used, and 22 synonymous substitutions were introduced into the first signal peptide to reduce the possibility of homologous recombination that could lead to a deletion of the entire insert (Fig. 1).

The bicistronic expression strategy allowed recovery of a mouse IFN-β-encoding virus that was capable of producing high levels of the IFN in Vero cells, which are defective in the synthesis of endogenous (monkey) IFN-β (33). Forty-eight hours after infection with MVEV.IFN-β, Vero cells produced more than 400 ng/ml of recombinant mouse IFN-β, whereas no IFN-β was detectable in the culture fluid from Vero cells infected with MVEV.C-IRES (Fig. 2A). The virus-produced IFN-β was biologically active: pretreatment of wild-type B6 MEFs with a 10^3-fold dilution of a supernatant harvested from MVEV.IFN-β infected Vero cells at 48 h p.i. inhibited the growth of *Semliki Forest virus* by $>10^6$-fold in comparison to control supernatants harvested from MVEV.C-IRES-infected Vero cells (Fig. 2B).

Growth of bicistronic viruses in cultured cells. MVEV.C-IRES and MVEV.IFN-β produced plaques on Vero cells that were of similar size but smaller than those for MVEV.wt (Fig. 3A). Further characterization revealed that both bicistronic viruses multiplied in Vero cells with similar kinetics and reached similar virus titers (Fig. 3B). While the growth kinetics of both viruses were somewhat slower than that of the parental virus, comparable peak viral titers were eventually achieved. In sharp contrast, the growth of MVEV.IFN-β was completely abolished in B6 MEFs (Fig. 3C) and in mouse L929 cells (data not shown), while MVEV.C-IRES produced 10- to 100-fold-lower titers in B6 MEFs and L929 cells in comparison to MVEV.wt over the course of the growth experiment. Coinfection of B6 MEFs with wild-type and IFN-β-encoding MVEV initially reduced the yield of infectious virus in the culture medium by >10-fold relative to infection with MVEV.wt alone, but titers continued to rise beyond 24 h p.i. However, despite using a slightly higher multiplicity of infection, titers in coinfection experiments never reached wild-type levels.

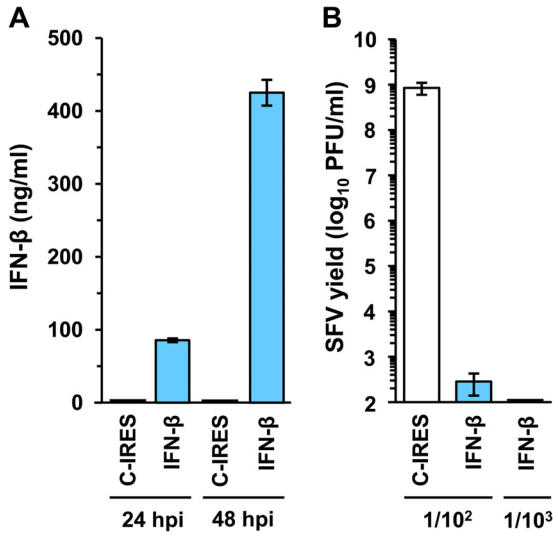

FIG 2 Recombinant IFN expression from a bicistronic flavivirus. (A) Vero cells grown in 6-well culture trays (5×10^5 cells/well) were infected with MVEV.IFN-β (IFN-β) or the control virus MVEV.C-IRES (C.IRES) at a multiplicity of 5 PFU per cell. At 24 h p.i., the entire culture supernatant (1 ml) was harvested and replaced with 1 ml of fresh medium, a second harvest was taken at 48 h p.i., and the IFN-β protein concentration in both samples was determined by ELISA. Means from 2 samples ± standard deviations (SD) are presented. (B) Wild-type B6 MEFs in 6-well culture trays (5×10^5 cells/well) were treated for 16 h with 1.5 ml of 10^2- or 10^3-fold dilutions of UV-inactivated culture fluid that was harvested 48 h p.i. from Vero cells infected with MVEV.IFN-β or MVEV.C-IRES. After this pretreatment, MEFs were infected with *Semliki Forest virus* (multiplicity of infection of ~1), and 24 h later, virus yields were measured by plaque titration on Vero cells. Means from 3 samples ± SD are presented.

We concluded that the growth restriction of MVEV.IFN-β in B6 MEFs and L929 cells was due to the ability of these cells to mount an effective antiviral state in response to mouse IFN-β, because MEFs from IFNAR$^{-/-}$ mice supported the growth of the IFN-coexpressing virus to titers that were only marginally (~2-fold) lower than those for MVEV.C-IRES (Fig. 3D). The growth of both bicistronic viruses in the IFN response-defective MEFs was markedly reduced relative to that of MVEV.wt, as was observed in MEFs from wild-type B6 mice.

Together the results show that coexpression of IFN-β potently restricts flavivirus growth in cells that are responsive to the cytokine. This suggests that IFN-β codelivery results in an abortive infection with MVEV.IFN-β and an antiviral state that restricts growth of coinfecting wild-type viruses. The data also demonstrate that bicistronic translation of a flaviviral genome (as with MVEV.C-IRES) *per se* affects virus replication in IFN-competent mouse cells but has only a marginal inhibitory effect on virus growth in Vero cells. The latter is important in terms of a translational application of the bicistronic flaviviruses, since it demonstrates that high-titer recombinant virus stocks can be generated in Vero cells, a cell line that is suitable for the production of vaccines and other therapeutic reagents.

Genetic stability of bicistronic MVEV. Ten consecutive passages of MVEV.C-IRES in Vero cells did not result in deletion of

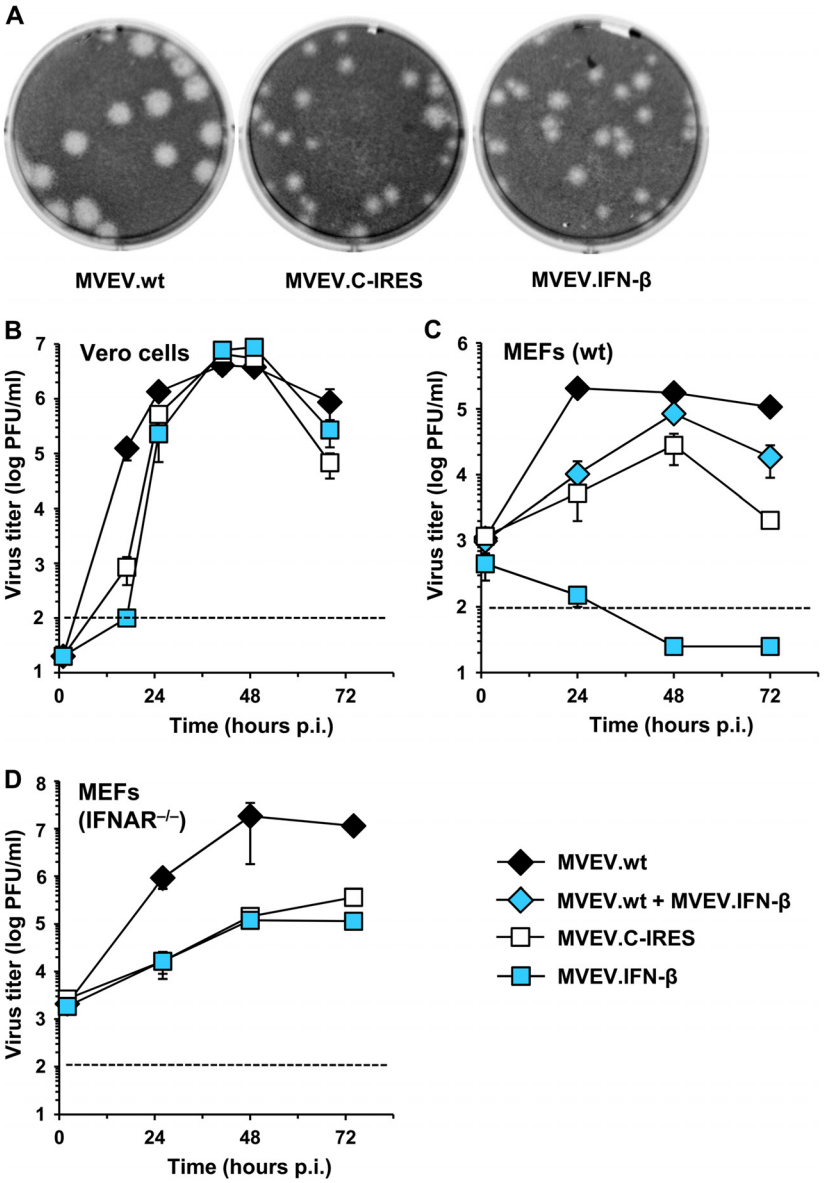

FIG 3 Growth of MVEV.wt and two bicistronic MVEV-based viruses in cell culture. (A) Plaque morphologies for MVEV.wt, MVEVC.IRES, and MVEV.IFN-β on Vero cell monolayers. (B, C, and D) Growth kinetics in Vero cells, IFN-sufficient (wt), and defective ($IFNAR^{-/-}$) MEFs, respectively. Cells were infected at a multiplicity of infection of 0.1 (Vero), 1 (wt MEFs), or 0.2 ($IFNAR^{-/-}$ MEFs); in a double-infection experiment (blue diamonds), MEFs were simultaneously infected with MVEV.wt and MVEV.IFN-β (with a multiplicity of infection of 1 for each virus). Virus titers in the cell culture fluid were determined by plaque titration on Vero cells. The dotted lines denote the detection limit of virus yield by plaque assay. The mean titers ± standard errors of the means (SEM) from two independent experiments are shown.

the IRES (data not shown), while serial passage of MVEV.IFN-β showed that both the IFN gene and IRES were maintained in the recombinant genome over at least 7 passages (Fig. 4). Moreover, all of the 12 plaque-purified viruses derived from passage 7 produced detectable amounts of IFN-β upon infection of a fresh Vero cell monolayer. Sequence analysis of the IFN gene in plaque-purified passage 7 viruses revealed no mutations, consistent with the notion that there is no particular evolutionary pressure on the IFN transgene in cells that do not respond to the heterologous IFN being made (most IFNs act in a species-specific manner, and mouse IFN-β does not induce signaling in Vero cells). However, after three further passages, major genome heterogeneity appeared, as exemplified by the detection of an RT-PCR amplicon only slightly larger than that for the wild-type virus (Fig. 4B, compare lanes 1 and 7). Sequence analysis of the amplicon showed almost complete reversion to the wild-type virus sequence, except for the presence of an additional 14 amino acids at the N terminus of the prM protein, which corresponded to the N-terminal 14 amino acids of IFN-β (INYKQLQLQERTNI). This finding points to a suitable insertion site for foreign, albeit small, polypeptides into the flavivirus polyprotein. We also performed 5 consecutive passages of MVEV.IFN-β in MEFs from B6 mice to test whether in the context of an abortive infection in the IFN-responsive cells the extreme selection pressure would result in loss of functional IFN

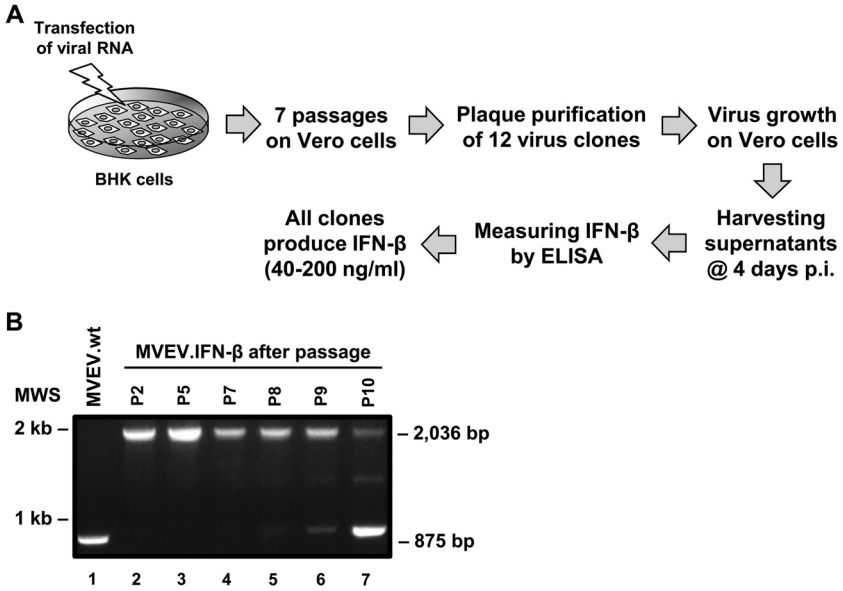

FIG 4 Genome stability of MVEV.IFN-β after serial passaging. (A) Schematic diagram of the experimental setup to measure the genetic stability of MVEV-.IFN-β. (B) Electrophoresis profiles of RT-PCR products of MVEV.wt (lane 1) and MVEV.IFN-β after cell passages 2, 5, 7, 8, 9, and 10 (lanes 2 to 7, respectively). Positions of marker bands and expected product sizes are shown on the left and right, respectively.

expression and a complete or partial restoration of virus growth. However, no infectious virus was recovered from the culture supernatants of this passage series.

Virulence attenuation of bicistronic MVEV. Three different mouse models were used to assess the virulence of bicistronic MVEV in the presence and absence of IFN-β coexpression: (i) weanling mice, (ii) severely immunocompromised (NOD-*scid*) mice, and (iii) type I IFN response-deficient ($IFNAR^{-/-}$) mice.

(i) Weanling mice. MVEV is highly neuroinvasive (as measured by mortality rate after extraneural infection). The 50% lethal doses (LD_{50}) of wild-type isolates and infectious clone-derived MVEV in weanling mice correspond to only 10 to 100 PFU (as measured in Vero cells) when inoculated by the i.p. route and do not exceed by more than 10-fold the LD_{50} following intercranial (i.c.) injection of viruses (22, 34). The neuroinvasiveness of MVEV decreases in adult mice, while neurovirulence (mortality rate after i.c. infection) is not strictly age dependent (23). We found that both bicistronic MVEVs were highly attenuated in both neuroinvasiveness and neurovirulence (Table 1). The i.p. LD_{50} of MVEV.IFN-β could not be determined but is expected to exceed that of the wild-type virus by more than 10,000-fold (i.e., no mortality was observed even at the highest dose, 10^5 PFU), while MVEV.C-IRES produced some mortality (40%, 4 out of 10 mice) in mice that were infected with 10^5 PFU. Furthermore, i.c. infection of mice with 10^3 PFU of either of the bicistronic viruses did not result in any mortality, which contrasted with an i.c. LD_{50} of only 1 to 10 PFU for the wild-type virus (22). An i.c. dose of 10^4 PFU was lethal in a small number of animals, again with a higher number of deaths in animals infected with MVEV.C-IRES than in animals infected with MVEV.IFN-β (3 and 1 out of 14 mice, respectively) (Table 1).

(ii) Severely immunocompromised mice. Given the high level of virulence attenuation of the bicistronic viruses in weanling mice, we next examined whether they were also attenuated in severely immunocompromised animals (Fig. 5A). Adult NOD-*scid* mice that lack functional B and T cells were challenged with 10^3 or 10^5 PFU of MVEV by the i.v. route; all mice succumbed to MVEV.wt infection by day 12 and day 9, respectively, while a dose response in mortality rate was clearly apparent for the bicistronic viruses. Notably, all animals infected with 10^3 PFU of MVEV.IFN-β survived past 28 days, and infection with 10^3 PFU of MVEV.C-IRES resulted in the death of only one out of 8 mice. Infection with 10^5 PFU resulted in 67% and 90% mortality for MVEV.IFN-β and MVEV.C-IRES, respectively. Accordingly, we again saw a trend of decreased virulence as a result of IFN coexpression, although this did not reach statistical significance with the number of NOD-*scid* mice used.

(iii) Type I IFN receptor-deficient mice. Knockout mice that lack a functional type I IFN response are highly susceptible to many viruses, including MVEV; even a relatively small virus inoculum (10^2 PFU delivered by an extraneural route) results in a fulminating infection, high viral loads in extraneural tissues and in the central nervous

TABLE 1 Neuroinvasiveness and neurovirulence in weanling BALB/c mice[a]

Virus	Route of infection	Dose (PFU)	Mortality (%)	Avg survival time (days) ± SD
MVEV.wt	i.p.	1,000	17/17 (100)	7.9 ± 1.4
		100	4/5 (80)	10.0
		10	2/5 (40)	8.0
MVEV.C-IRES		100,000	4/10 (40)	9.0
		10,000	0/5 (0)	
		1,000	0/5 (0)	
MVEV.IFN-β		100,000	0/10 (0)	
		10,000	0/5 (0)	
		1,000	0/5 (0)	
MVEV.C-IRES	i.c.	10,000	3/14 (21)	8.3 ± 0.6
		1,000	0/5 (0)	
MVEV.IFN-β		10,000	1/14 (7)	9.0
		1,000	0/5 (0)	

[a] Groups of 23- to 27-day-old male or female BALB/c mice were infected i.p. or i.c. with the given virus doses, and morbidity and mortality were monitored over a period of 14 days. The data were compiled from 5 experiments.

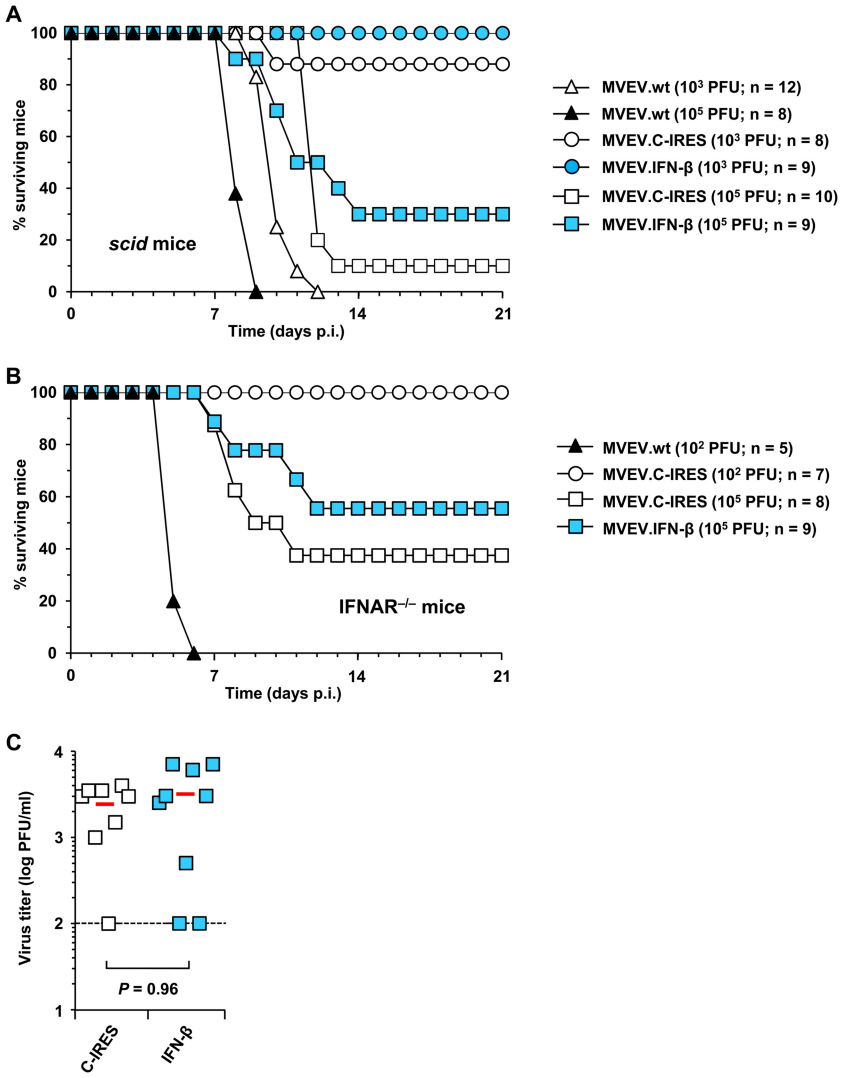

FIG 5 Virus attenuation in immunodeficient mice. (A and B) Groups of 6- to 7-week-old NOD-*scid* mice or 6- to 8-week-old IFNAR$^{-/-}$ mice were infected with 10^3 to 10^5 PFU i.v. (*scid* mice) or 10^2 to 10^5 PFU i.p. (IFNAR$^{-/-}$ mice) of MVEV.wt, MVEV.C.IRES, or MVEV.IFN-β. Mice were monitored daily for a period of 28 days and morbidity and mortality were recorded. (C) At 2 days p.i., sera were collected from MVEV.C-IRES ($n = 8$)- and MVEV.IFN-β ($n = 9$)-infected IFNAR$^{-/-}$ mice and viremia titers determined by plaque assay on Vero cells. Each symbol represents an individual mouse, and mean titers are indicated by a horizontal red line. The dotted line represents the detection limit of the plaque assay.

system (CNS), and rapid and uniform mortality (35). In contrast to the high virulence of MVEV.wt in IFNAR$^{-/-}$ mice, MVEV.C-IRES did not cause mortality in a group of mice challenged with 10^2 PFU i.p. (Fig. 5B). Challenges with a much higher virus dose (10^5 PFU, i.p.) of MVEV.IFN-β or MVEV.C-IRES killed only a proportion of IFNAR$^{-/-}$ mice (Fig. 5B). The result demonstrates strong but not complete attenuation of both bicistronic viruses in mice that lack a functional type I IFN system. The virulences of MVEV.IFN-β and MVEV.C-IRES as assessed by mortality rate and viremia at day 2 p.i. did not differ significantly (Fig. 5B and C), a result that is consistent with the comparable growth properties of the bicistronic viruses in mouse IFN-β response-deficient Vero cells and MEFs from IFNAR$^{-/-}$ mice (Fig. 3).

Collectively, the data show that bicistronic flaviviral genome organization provides a remarkable degree of attenuation of virulence that is exemplified by the recovery of weanling mice from high-dose i.c. infections and the survival of severely immunocompromised mice from challenges with virus doses that are uniformly lethal for wild-type MVEV. Furthermore, the result of a meta-analysis (Table 2) demonstrates a further, statistically significant reduction in virulence when IFN-β is coexpressed.

Viral burden in the CNS is reduced by IFN-β coexpression. We also examined virus growth and spread in the CNS of weanling mice after i.c. infection with 10^3 PFU of either MVEV.wt, MVEV-C.IRES, or MVEV.IFN-β. For these experiments, we used congenic BALB.A2G-*Mx1* mice that are genetically and phenotypically very similar to standard BALB/c mice but carry the wild-type *Mx1* allele of A2G mice. While the IFN-induced, antiviral nuclear molecule Mx1 does not contribute to suppression of flaviviral infection (36), it is a sensitive biomarker for measuring type I IFN responses (see below). Mice were killed at different times p.i., and whole-brain sections cut from the right hemisphere were stained for the presence of the MVEV NS1 protein as a correlate of infection levels. NS1 is an intracellular,

TABLE 2 Meta-analysis of virus attenuation

Virus	Mortality (%)[a]					
	Weanling[b] mice		*scid* mice		IFNAR$^{-/-}$ mice, i.p. (10^5)	Combined (all models)
	i.c. (10^3)	i.p. (10^5)	i.v. (10^3)	i.v. (10^5)		
MVEV.C-IRES	3/14 (21)	4/10 (40)	1/8 (13)	9/10 (90)	5/8 (63)	22/50 (44)[c]
MVEV.IFN-β	1/14 (7)	0/10 (0)	0/9 (0)	7/9 (78)	4/9 (44)	12/51 (24)

[a] Data were taken from Table 1 and Fig. 5. The route of infection and virus dose (PFU) are indicated.
[b] Mouse model.
[c] $P = 0.036$ by the two-tailed Fisher exact test.

cell surface, and secreted nonstructural flavivirus protein; therefore, it cannot be excluded that in a severe infection of the brain some NS1-specific staining might be the result of attachment or uptake of NS1 into uninfected cells. In animals infected with MVEV.wt, we observed an exponential increase in the number of infected cells until mice succumbed to the virus by day 5 p.i. (Table 3). In contrast, we found only a small number of infected cells in the brains of mice that had been infected with the bicistronic viruses, with MVEV.C-IRES giving slightly more infected cells on days 4 and 7 p.i. than MVEV-.IFN-β.

We corroborated these findings by quantifying MVEV RNA in tissue samples taken from the left hemispheres of the same mice (Fig. 6A). The MVEV.wt genome content in brain increased exponentially with time, with titers in some mice reaching almost 10^{13} GEs/g of tissue (mean titer on day 4 p.i. $= 2.3 \times 10^{12}$ GEs/g). Significantly (~10,000-fold) less viral RNA accumulated in mice infected with MVEV.C-IRES, with peak titers at days 4 and 7 p.i. (mean $= 2.5 \times 10^8$ and 2.8×10^8 GEs/g, respectively). At later times, RNA levels decreased, pointing to a recovery from the infection (mean titers at day 16 p.i. showed an ~100-fold decrease compared to peak levels). Brains from mice infected with MVEV.IFN-β showed barely detectable levels of viral RNA, with only one animal presenting with a titer that exceeded 10^6 GEs/g tissue. Taken together, the data substantiate the finding that both bicistronic flaviviruses are highly attenuated, and they lend further support to the concept of additional suppression of viral growth and virulence by the codelivery of IFN-β.

Coexpression of IFN stimulates a robust innate immune response in the CNS despite abortive virus replication. Having demonstrated the excellent safety profile of MVEV.IFN-β, we next analyzed organ-wide expression levels and biological activity of the coexpressed cytokine. Given that MVEV is neurotropic in the mammalian host, the parameters were evaluated in brains of mice infected by the i.c. route. At first we analyzed the expression of IFN-β by quantitative PCR and found, somewhat surprisingly, that IFN-β mRNA levels barely increased above baseline in brain tissue of mice infected with MVEV.IFN-β (Fig. 6B). This means that neither the transgene nor the endogenous gene produces substantial amounts of IFN-β, an observation that is in line with the fact that the viral load in MVEV.IFN-β-infected mice is extremely low. In sharp contrast, IFN-β mRNA levels increased dramatically in mice infected with MVEV.wt, which demonstrates that the CNS is capable of mounting a substantial IFN response against MVEV (if the virus load is high). Finally, mice infected with MVEV.C-IRES showed low but clearly detectable production of IFN-β mRNA, peaking at day 7 p.i., and with a time course that followed that of the virus load (Fig. 6A and B).

Measuring a low-level IFN response can be challenging. We addressed this problem by using BALB.A2G-*Mx1* instead of BALB/c mice, because Mx1 expression in these congenic mice can be used as a highly sensitive biomarker for the presence of type I/III IFNs (37) (reviewed in reference 38). We found that *Mx1* gene expression correlated well with that of IFN-β (Fig. 6C), with the highest levels of Mx1 mRNA found in mice infected with the wild-type virus, clearly elevated but relatively moderate levels in mice inoculated with MVEV.IFN-β, and intermediate levels in MVEV.C-IRES-infected mice. Interestingly, *Mx1* gene activity was still detectable in tissues of mice infected with MVEV.C-IRES at the end of the observation period (day 16 p.i.) but returned to near-baseline levels in 2 of 3 samples from the group of animals infected with MVEV.IFN-β (in line with previous findings on the kinetics of Mx expression in mice recovering from an RNA virus infection [39]).

Mx proteins accumulate in large, stable protein aggregates. With a half-life of more than 2 days (39, 40), Mx proteins can be used as a highly sensitive biomarker even for a fleeting and locally confined IFN production. To investigate the effect of flaviviral IFN coexpression on the IFN response at a cellular level in the CNS, double staining of brain sections for MVEV NS1 and IFN-induced Mx1 proteins was performed for subsequent immunohistochemical analysis (Fig. 7). As expected, we found widespread accumulation of both NS1 and Mx1 in mice infected with wild-type MVEV. In contrast, sections of brain from mice infected with the bicistronic viruses showed only very few cells that stained positive for NS1. However, notwithstanding the low number of detectable virus-infected cells, abundant Mx1 expression was observed, although the expression pattern was less homogeneous then in mice infected with MVEV.wt and was more variable between different regions of the brain and between individual mice. Notably, despite the lower number of NS1-positive cells in the CNS of mice infected with MVEV.IFN-β than in mice infected with MVEV.C-IRES (Table 3), IFN-β coexpression elicited comparable numbers of Mx1-expressing cells (Table 4).

Taken together, the results reinforce the notion that Mx1 protein expression can be used as an exquisitely sensitive marker for measuring the bioactivity of endogenous and recombinant IFNs. Moreover, the abundant accumulation of Mx1 protein in the CNS of mice infected with MVEV.IFN-β indicates efficient activation of the IFN response, despite an essentially abortive infection with a highly attenuated virus.

Immunogenicity of bicistronic MVEV. Neutralizing antibody is key both in recovery from primary flavivirus infection and in vaccine-mediated protection against flaviviruses (reviewed in references 18 and 19). Therefore, the humoral immune response elicited with the bicistronic viruses was compared to that with MVEV.wt in two mouse strains (B6 and BALB/c). Total anti-

TABLE 3 Attenuation of virus spread in the CNS

Virus[a]	Time (days p.i.)	Mouse	No. of infected cells (mean)/brain section[b]			
			Section area 1	Section area 2	Section area 3	Mean
MVEV.wt	1	B1-1	35	183	13	77
		B2-1	28	171	12	68
	2	B1-2	106	120	14	80
		B2-2	126	342	375	278
	4	B1-4	>1,000[c,d]	>1,000[c,d]	>1,000[c,d]	>1,000[c,d]
		B2-4	>1,000[c,d]	>1,000[c,d]	>1,000[c,d]	>1,000[c,d]
		B3-4	>1,000[c,d]	>1,000[c,d]	>1,000[c,d]	>1,000[c,d]
	7	B1-7	Died[d]			
		B2-7	Died[d]			
		B3-7	Died[d]			
MVEV.C-IRES	1	C1-1	0	0	0	0
		C2-1	0	0	0	0
	2	C1-2	2	0	0	1
		C2-2	0	0	0	0
	4	C1-4	37	118	22	59
		C2-4	1	0	1	1
	7	C1-7	2	2	5	3
		C2-7	9	3	4	5
	16	C1-16	0	0	1	0
		C2-16	0	0	0	0
MVEV.IFN-β	1	D1-1	1	0	0	0
		D2-1	0	0	0	0
		D3-1	2	0	0	1
	2	D1-2	0	1	0	0
		D2-2	1	0	0	0
		D3-2	0	0	0	0
	4	D1-4	2	1	1	1
		D2-4	1	0	2	1
		D3-4	1	0	0	0
	7	D1-7	0	0	0	0
		D2-7	0	0	0	0
		D3-7	1	0	0	0
	16	D1-16	0	2	0	1
		D2-16	0	0	0	0
		D3-16	0	0	0	0

[a] Groups of 3-week-old BALB.A2G-*Mx1* mice were i.c. inoculated with 10^4 PFU of MVEV.wt, MVEV.C-IRES, or MVEV.IFN-β, and groups of 2 or 3 mice were euthanized at the indicated time points for tissue collection.

[b] Sagittal brain sections (excluding cerebellum) were prepared and immune stained for the viral NS1 protein. For each section area (i.e., 1, 2, and 3), the number of cells with detectable antigen levels was determined by evaluating 2 neighboring sections of 4-μm nominal thickness. Section areas are separated by at least 250 μm. Sections from mock-treated control animals (inoculated with virus diluent only) were also examined, but as expected, no virus-infected cells could be identified (data not included).

[c] There were too many infected cells to count.

[d] All animals infected with MVEV.wt showed signs of disease at day 4 p.i. and either were killed or died the following night.

MVEV antibody titers and functional activity were determined by ELISA and neutralization assay, respectively (Table 5). The results showed that a two-dose vaccination schedule with MVEV.C-IRES induced a potent virus-specific antibody response and that the magnitude of the response reached levels similar to those obtained in mice infected with MVEV.wt. Moreover, the ELISA and $PRNT_{50}$ titers elicited with MVEV.IFN-β were only slightly lower than those achieved with MVEV.C-IRES. Booster immunizations given at 3 to 4 weeks after priming markedly enhanced the antibody response against the bicistronic viruses but not that against the wild-type virus. It should be noted that infections with MVEV.wt were severe and resulted in mortality rates of up to 60%, as reported previously (23). This complicates a direct comparison of antibody titers between wild-type and bicistronic viruses, because sterile immunity after priming with MVEV.wt most likely masked any booster effect of subsequent immunization in surviving mice.

Vaccine delivery by the i.m. route produced significantly higher antibody titers than that by the s.c. route for all immunogens and mouse strains tested (Table 5 and data not shown), while i.v. immunization of B6 mice with MVEV.IFN-β resulted in a further increase in ELISA and neutralizing antibody titers relative to those with the i.m. route (Table 5). We also noted that overall, the humoral immune response against MVEV was higher in B6 than in BALB/c mice and that the magnitude of the responses in prime-boost vaccination with MVEV.IFN-β was dose dependent, which is not the case for single i.v. infections with MVEV.wt in the dose range of 0.1 to 10^5 PFU (23).

Protective value of antibody responses elicited with bicis-

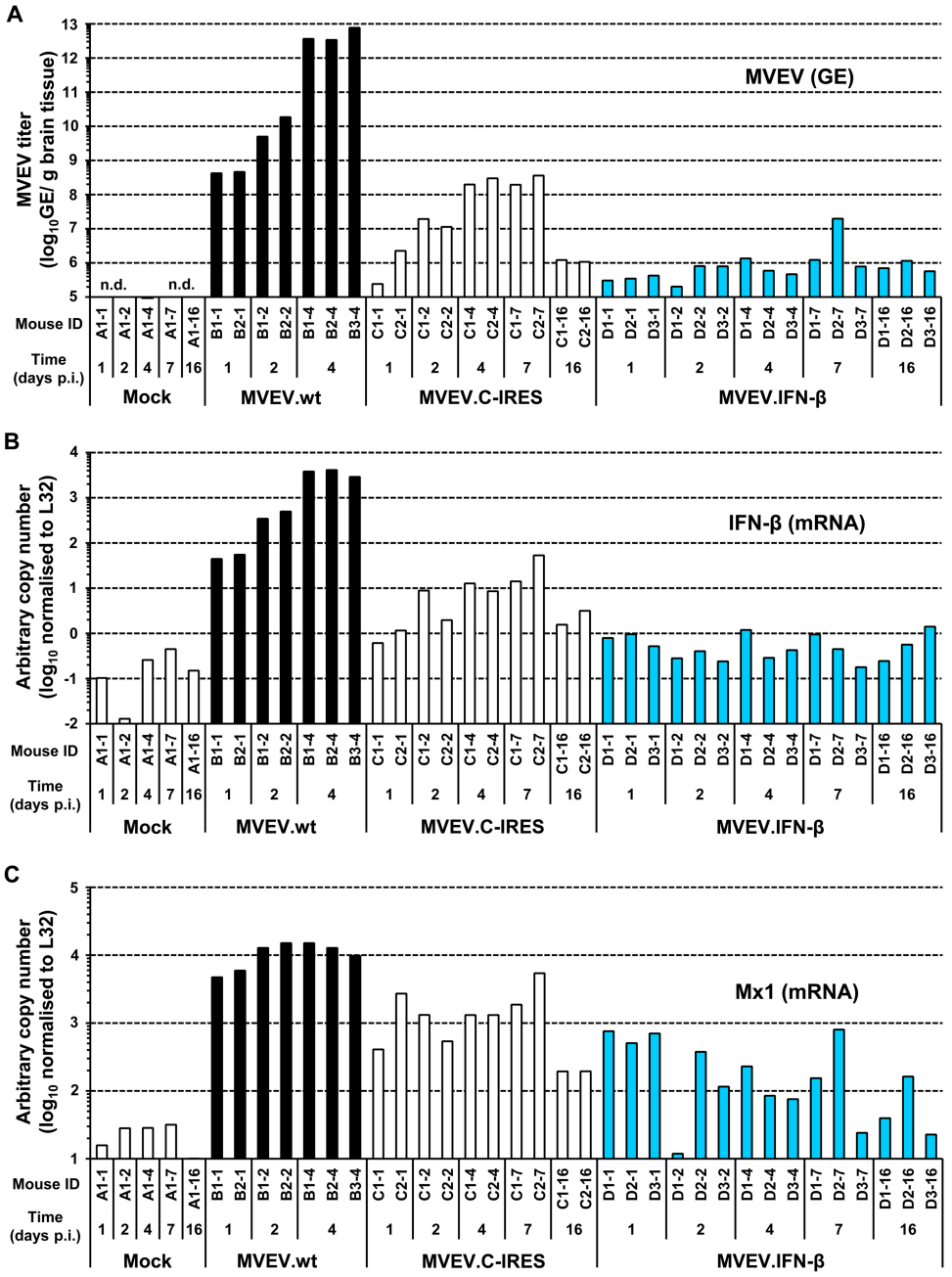

FIG 6 Virus RNA and innate immune mRNA quantification in the brain. BALB.A2G-*Mx1* mice (3 weeks old) were intracranially inoculated with 10^4 PFU of MVEV.wt, MVEV.C-IRES, or MVEV.IFN-β. Groups of 2 or 3 mice were killed at the time points indicated, and total RNA was isolated from a quarter of the brain. Quantitative RT-PCR was performed for MVEV RNA (A), IFN-β mRNA (B), and Mx1 mRNA (C). Bars represent mean values obtained from three independent quantitative PCRs (A) or are representative values chosen from two independent quantitative PCRs (B and C). GE, genome equivalent.

tronic MVEV. The protective efficacy of the humoral immune response elicited by vaccination with the bicistronic viruses was evaluated by adoptive transfer of immune B cells into 4-week-old B6 mice 1 day prior to a lethal challenge with MVEV.wt (Fig. 8). Given the low mortality rate in adult (>8-week-old) mice following extraneural infection with MVEV, young animals that are significantly more susceptible to the infection were used in the challenge experiment. B cells were isolated from donor mice at 9 weeks after the completion of a vaccination schedule consisting of two i.m. injections of 10^5 PFU of either of the bicistronic viruses and were transferred into recipient mice by the i.p. route. A subsequent infection with 10^5 PFU of MVEV.wt revealed that MVEV.IFN-β- and MVEV.C-IRES-immune B cells provided significant protection against disease in this stringent challenge model ($P = 0.02$ and 0.004, respectively, relative to naive B cell transfer). The result from this experiment clearly demonstrates the protective efficacy of a two-dose immunization regimen with bicistronic MVEVs, a finding that is consistent with a dominant role of B-cell memory in flavivirus vaccine protection (41, 42).

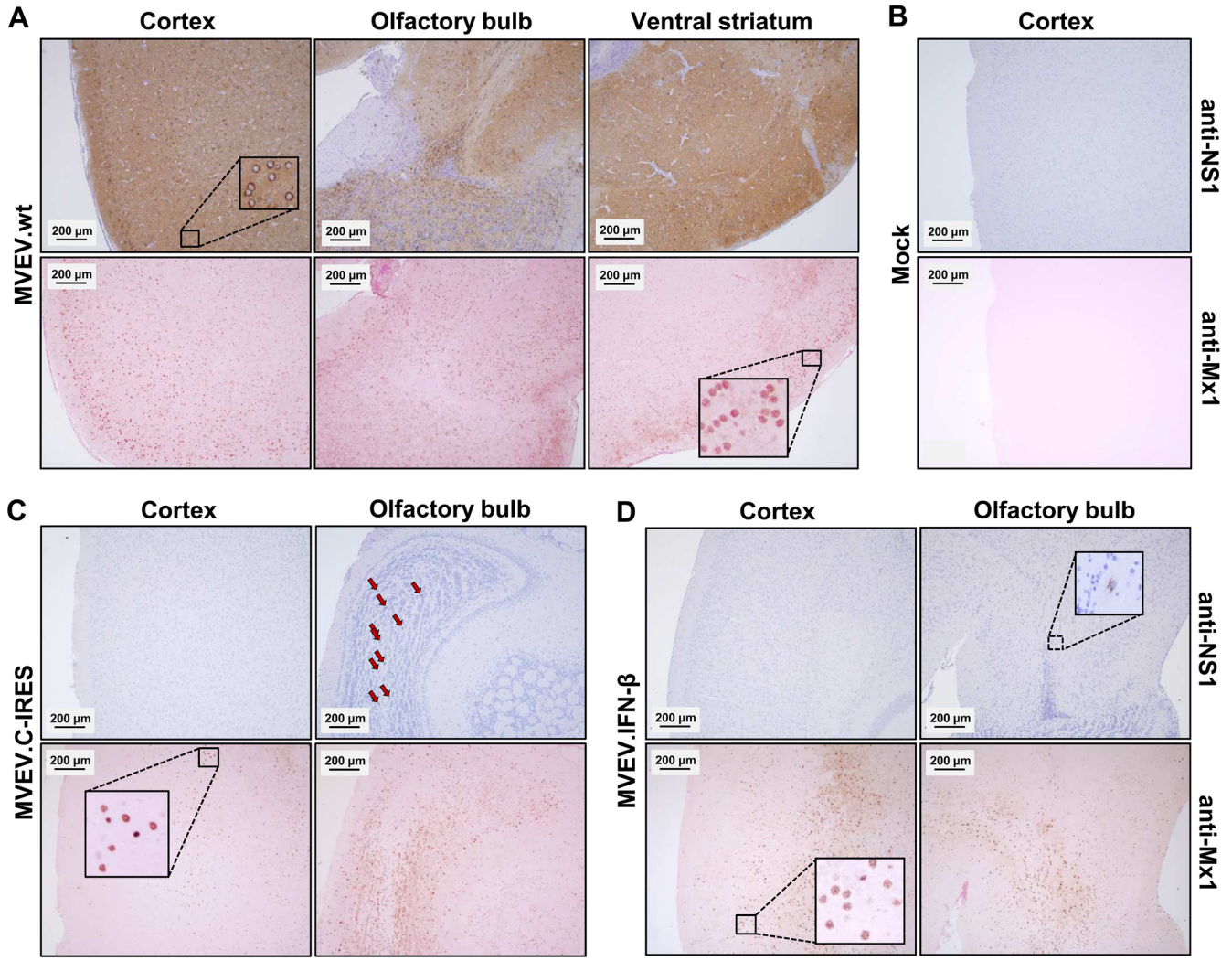

FIG 7 Virus and Mx1 protein accumulation in the brains of MVEV-infected mice. Adult BALB.A2G-*Mx1* mice were intracranially inoculated with 10^4 PFU of MVEV.wt (mouse B1-4) (A), diluent alone (mock, mouse A1-1) (B), MVEV.C-IRES (mouse C1-4) (C), and MVEV.IFN-β (mouse D1-4) (D). Mice were killed at 4 days p.i., 4-μm sagittal brain sections were prepared, and neighboring sections were immunostained for the virus protein NS1 (anti-NS1) or Mx1 (anti-Mx1). Sections were then counterstained using either hematoxylin (together with anti-NS1) or eosin (with anti-Mx1). Insets show the typical cytoplasmic and nuclear staining patterns of NS1 and Mx1, respectively. Arrows point to a number of NS1-positive cells in the olfactory bulb of mouse C1-4. Bars, 200 μm.

DISCUSSION

We have devised a novel bicistronic genome organization for an IRES-based attenuation of flavivirus vaccine candidates. Our strategy exploited a flavivirus unique polyprotein-processing mechanism at the junction of the viral C and prM proteins. The two proteins are separated by a signal peptide, and it was previously shown that cleavage at the cytosolic side of the signal peptide by the viral NS2B-3 protease produces the mature C protein and triggers efficient ER luminal signalase cleavage of prM (43, 44). It is thought that this coordination of cleavage events at the C-prM protein junction promotes efficient virus morphogenesis (25, 45). Disruption of the obligatory sequence of cleavages by introduction of three point mutations into the signal peptide produced a mutant virus that showed significantly poorer growth in cell culture and virulence attenuation in mice (45); it also accounted for loss of flavivirus-induced upregulation of major histocompatibility complex (MHC) class I at the cell surface (46), a phenomenon that may provide a strategy for flavivirus immune escape from the natural killer (NK) cell response (47, 48). The bicistronic MVEV.C-IRES genome is translated to produce mature C protein following 5′-cap-dependent initiation of translation, while synthesis of all other viral proteins is driven by an IRES at the C-prM gene junction. This results in the uncoupling of the coordinated cleavages at the C-prM junction. Accordingly, the IRES-based attenuation of a flavivirus described in this study involves at least two mechanisms that putatively reduce viral virulence: (i) suboptimal viral protein levels and/or an imbalance of the relative amounts of virus proteins and (ii) suboptimal virus assembly. Moreover, increased size and altered genome secondary RNA structures may have also contributed to the reduced growth efficiency of recombinant bicistronic viruses.

Safety and immunogenicity are key parameters that determine the suitability of live virus vaccines. The bicistronic flavivirus candidate vaccine (MVEV.C-IRES) showed a remarkable level of vir-

TABLE 4 Mx protein quantification in the brain

Virus[a]	Time (days p.i.)	Mouse ID	Mx expression[b]
Mock	1	A1-1	−
	7	A1-7	−/+
MVEV.wt	1	B1-1	++
		B2-1	++
	2	B1-2	++
		B2-2	+++
	4	B1-4	++++
		B2-4	++++
		B3-4	++++
	7	B1-7	Died[c]
		B2-7	Died[c]
		B3-7	Died[c]
MVEV.C-IRES	1	C1-1	+
		C2-1	++
	2	C1-2	++
		C2-2	+
	4	C1-4	++
		C2-4	−/+
	7	C1-7	+
		C2-7	+
	16	C1-16	++
		C2-16	++
MVEV.IFN-β	1	D1-1	+
		D2-1	+
		D3-1	+
	2	D1-2	+
		D2-2	++
		D3-2	+
	4	D1-4	++
		D2-4	+
		D3-4	+
	7	D1-7	+
		D2-7	++/+++
		D3-7	−/+
	16	D1-16	−/+
		D2-16	+/++
		D3-16	+

[a] Groups of 3-week-old BALB.A2G-*Mx1* mice were i.c. inoculated with 10^4 PFU of MVEV.wt, MVEV.C-IRES, or MVEV.IFN-β and euthanized at the indicated time points for tissue collection.

[b] Sagittal brain sections (excluding the cerebellum) were prepared, immunostained for Mx proteins, and examined microscopically. The number of Mx-expressing cells and the amount of Mx protein within a given cell were determined in a semiquantitative manner: −, no positive cells; −/+, individual or small groups of positive cells (nuclear staining only); +, larger groups of positive cells; ++, even larger groups of positive cells in relatively confined areas; +++, large number of positive cells in confluent areas (nuclear plus weak cytoplasmic staining); ++++, almost all nuclei at least weakly positive and large confluent areas with strongly positive nuclei (plus weak to moderate cytoplasmic staining).

[c] All animals infected with MVEV.wt showed signs of disease at day 4 p.i. and were either killed or died the following night.

ulence attenuation while retaining potent immunogenicity. It displayed an ~10,000-fold reduction of neuroinvasiveness and at least a 1,000-fold reduction in neurovirulence in weanling mice, a model commonly used for flavivirus virulence determination. Notably, the i.c. LD_{50} for MVEV.C-IRES was >1,000-fold lower than that of the yellow fever 17D vaccine, the gold standard for a successful live-attenuated flavivirus vaccine; the i.c. LD_{50} of the yellow fever vaccine in weanling BALB/c mice is ~1 (our unpublished result). MVEV.C-IRES was also highly attenuated in immunodeficient mice defective in either adaptive (NOD-*scid*) or innate ($IFNAR^{-/-}$) immune responses. Nevertheless, the high level of attenuation did not prevent efficient induction of humoral immunity, the immune response that is pivotal in vaccine protection against flaviviruses (18, 19). Using a two-dose vaccination regimen, all mice developed neutralizing antibody responses of a magnitude exceeding that considered protective ($PRNT_{50} \geq 10$) in the case of the closely related *Japanese encephalitis virus* (49) and similar to levels found in mice infected with MVEV.wt. It is thought that survivors of a natural flavivirus infection acquire life-long protective immunity against that virus. Accordingly, we speculate that immunization with MVEV.C-IRES will also durably protect against disease following exposure to MVEV. Using immune B cell transfer from MVEV.C-IRES-immunized mice to young recipients that were lethally challenged with MVEV, we confirmed the *in vivo* protective efficacy of the vaccine and also demonstrated that the vaccine induced protective memory B cells in addition to neutralizing antibody. Finally, genome stability, in addition to a high level of virulence attenuation, is a critical safety parameter for a live bicistronic flavivirus vaccine. MVEV.C-IRES showed high genome stability without evidence of reversion to a monocistronic genome organization in a prolonged cell culture passaging series. These findings collectively highlight the potential of the IRES-based attenuation approach in flavivirus vaccine development.

This study also investigated the effect of coexpression of IFN-β on vaccine properties of a bicistronic MVEV. IFN-β is an "immediate early IFN" that signals predominantly in an autocrine and paracrine manner, thereby promoting the subsequent expression of a wider array of IFN-α subtypes (8). We posited that earlier and/or increased production of type I IFN at the infection site would restrict dissemination of the IFN-encoding virus but also stimulate the generation of adaptive immune responses against viral antigens. MVEV.IFN-β, the first flavivirus encoding a cytokine/IFN, produced high levels of IFN (~400 ng/ml at 2 days p.i.) in Vero cells, a monkey cell line that is nonresponsive to mouse IFN-β. Growth of the IFN-encoding bicistronic MVEV in Vero cells was comparable to that of a bicistronic MVEV lacking the IFN-β gene and only marginally poorer than that of MVEV.wt. However, in IFN-responsive cells, MVEV.IFN-β produced a virtually abortive infection. Interestingly, we found that both bicistronic MVEVs were much more attenuated than the wild-type virus in $IFNAR^{-/-}$ MEFs, while all three viruses replicated to similar levels in Vero cells, an observation that probably reflects differences in the innate immune competence of the two cell culture systems. $IFNAR^{-/-}$ MEFs lack a functional IFN-α/β receptor, but alternative IFN signaling may still occur (50), while Vero cells lack the ability to produce type I IFNs (33) and do not respond to mouse IFNs due to the species-specific binding of IFNs to their respective receptors (51).

The IFN-encoding bicistronic MVEV showed high but not absolute genome stability. Only after prolonged passaging in Vero cells was there a loss of IFN expression and deletion of foreign sequences from the MVEV genome; passaging of MVEV.IFN-β in IFN-responsive cells did not result in the appearance of revertant viruses lacking IFN expression, most likely as a consequence of the self-limiting replication of the recombinant virus in these cells. The results confirm that the use of a novel insertion site at the

TABLE 5 MVEV-specific antibody responses[a]

Mouse strain	Virus	Dose (PFU)	Route	No. of animals/group	Mean $\log_{10}$ antibody titer (SD)[b]		Mean $PRNT_{50}$ titer (range)[c]	
					First bleed	Second bleed	First bleed	Second bleed
C57BL/6	MVEV.wt[d]	10^3	i.m.	2	4.2 (0.4)	4.1 (0.6)	320 (pool)	60 (40–80)
	MVEV.C-IRES	10^5		10	4.0 (0.3)	4.7 (0.3)	40 (pool)	192 (80–320)
	MVEV.IFN-β	10^5		10	2.5 (0.5)	3.7 (0.4)	10 (pool)	50 (<10–80)
	MVEV.wt[e]	10^3	i.v.	4	4.0 (0.2)	4.3 (0.2)	160 (pool)	120 (80–160)
	MVEV.IFN-β	10^3		5	<2.0	2.6 (0.6)	<10 (pool)	<10 (pool)
	MVEV.IFN-β	10^5		5	4.0 (0.1)	5.3 (0)	10 (pool)	180 (80–320)
BALB/c	MVEV.wt[f]	10^5	i.m.	6	3.6 (0.3)	4.2 (0.1)	20 (pool)	113 (40–160)
	MVEV.C-IRES	10^5		10	2.8 (0.4)	4.3 (0.4)	10 (pool)	82 (20–160)
	MVEV.IFN-β	10^5		10	2.5 (0.3)	4.2 (0.3)	<10 (pool)	15 (<10–40)
	MVEV.wt	10^5	s.c.	10	NT[g]	3.3 (0.3)	NT	20 (pool)
	MVEV.C-IRES	10^5		10	NT	3.7 (0.3)	NT	20 (pool)
	MVEV.IFN-β	10^5		10	NT	3.1 (0.1)	NT	<10 (pool)

[a] Groups of 7- to 8-week-old C57B6 or BALB/c mice were immunized with wild-type or recombinant MVEV using the dose and route indicated and were boosted with the same dose and by the same route 3 to 4 weeks later. Sera were collected prior to delivery of the booster dose and at 3 to 4 weeks after the second immunization.
[b] ELISA endpoint titers of individual test sera were determined as described in Materials and Methods section.
[c] Plaque reduction neutralization by individual or pooled test sera against MVEV were determined as described in Materials and Methods.
[d] Three mice succumbed to MVEV.wt infection; the indicated group size represents surviving mice.
[e] One mouse succumbed to MVEV.wt infection; the indicated group size represents surviving mice.
[f] Four mice succumbed to MVEV.wt infection; the indicated group size represents surviving mice.
[g] NT, not tested.

C-prM junction significantly improves recombinant bicistronic flavivirus genome stability in comparison to highly unstable insertion sites in the 3′ untranslated region that were previously employed (52–54). This indicates the suitability of a new generation of recombinant bicistronic flavivirus vectors for clinical use in applications that do not require prolonged virus replication, such as vaccinations. Our approach of inserting an IRES at the C-prM junction differs from previous attempts to generate replication-competent bicistronic flaviviral genomes in which an IRES was placed between the 5′ promoter element and the start of the viral polyprotein sequence (55, 56).

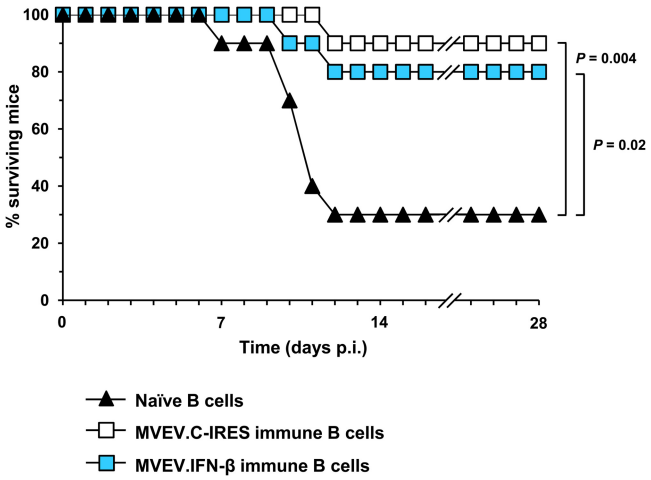

FIG 8 Protection against lethal challenge with MVEV. B6 donor mice (10 mice/group) were immunized (i.m.) with two doses of 10^5 PFU of either MVEV.C-IRES or MVEV.IFN-β, delivered 3 weeks apart (Table 3), and B cells were isolated at 9 weeks after completion of the vaccination schedule and adoptively transferred into 4-week-old recipients ($n = 10$/group). Additionally, B cells from naive mice were transferred into control mice ($n = 10$). One day after the transfer, mice were challenged with 10^5 PFU of MVEV.wt by footpad injection and monitored twice daily for morbidity and mortality for 28 days.

The virulence of MVEV.IFN-β in mice was highly attenuated, albeit with a level of attenuation that was only slightly greater than that of the bicistronic control virus, MVEV.C-IRES. This was perhaps not unexpected, given the already high level of attenuation observed for the IRES-based vaccine candidate. A comparison of the immunogenicity and protective value against lethal challenge with MVEV in mice between MVEV.IFN-β and MVEV.C-IRES showed that the marginally lower virulence found when IFN-β was coexpressed came at the cost of a slightly reduced vaccine efficacy. These results raised the question of whether the codelivery of IFN-β resulted in overattenuation and if the choice of a different IFN with lower antiviral activity would have more convincingly uncovered an immune-potentiating adjuvant effect of the cytokine. Although all type I IFNs bind to a common receptor complex, binding properties and biological activities of individual IFNs (even those of closely related subtypes) may vary dramatically (see, e.g., reference 57). Thus, type I IFNs other than IFN-β or more distantly related IFN such as type III IFNs may provide a more optimal balance of attenuation and immunogenicity, as was reported for poxviral codelivery of several IFNs (13). Given that viruses differ in their sensitivity to different IFN types and subtypes (58, 59) and that adaptive immune responses vary in their protective value against different viruses, it is likely that using the IFN coexpression strategy in vaccination will require a virus-specific optimization of IFN subtype.

Finally, we examined whether delivery of IFN-β and/or triggering of IFN responses could be accomplished in the CNS by the inoculation of MVEV.IFN-β. The brain was chosen as a target organ, because MVEV is neurotropic and replicates poorly in extraneural tissues. Overall, we found that (endogenous) IFN-β

gene expression in infected brains strictly correlated with virus replication and that the poor replication of MVEV.IFN-β prevented consistent detection of above-baseline IFN-β mRNA levels. For increased sensitivity, we used the IFN-stimulated gene *Mx1* as a sensitive biomarker for type I IFNs, and indeed we could detect an increase in Mx1 mRNA levels in most animals between 1 and 7 days p.i. A detailed analysis of the IFN response at the cellular level (via Mx1 protein detection) showed a patchy distribution of Mx1 expression throughout the brains of MVEV.IFN-β infected mice, which was markedly more widespread than that of viral antigen-positive cells. Furthermore, the expression pattern was comparable for the IFN-β-encoding virus and MVEV.C-IRES, although the latter grew to higher titers, suggesting that transgene expression boosted the IFN-production in the CNS of mice infected with MVEV.IFN-β. In sharp contrast, a much more widespread and homogeneous expression of Mx1 was observed in brains of mice infected with MVEV.wt. Thus, the MVEV backbone is perhaps poorly suited for therapeutic delivery of IFN-β because its replication is too sensitive to the coexpressed cytokine. However, further research might show the suitability of flavivirus-vectored delivery of other IFN types/subtypes or that of alternative backbones for a more robust IFN-β expression in the CNS.

Taken together, our results with MVEV suggest that a bicistronic virus design and the coexpression of IFN can be employed to further increase the safety of flavivirus vaccine candidates.

ACKNOWLEDGMENTS

We thank Georg Kochs for the Mx-specific antibody M143, Peter Staeheli for Mx1-congenic mice, and Kerry Mills for a critical reading of the manuscript. We are grateful to Paivi Lobigs, Helen Taylor, and Jill Medveczky for excellent technical assistance.

M.F. and I.R. received support from BioDiem Ltd.

REFERENCES

1. **Coleman JR, Papamichail D, Skiena S, Futcher B, Wimmer E, Mueller S.** 2008. Virus attenuation by genome-scale changes in codon pair bias. Science **320:**1784–1787. http://dx.doi.org/10.1126/science.1155761.
2. **Yang C, Skiena S, Futcher B, Mueller S, Wimmer E.** 2013. Deliberate reduction of hemagglutinin and neuraminidase expression of influenza virus leads to an ultraprotective live vaccine in mice. Proc. Natl. Acad. Sci. U. S. A. **110:**9481–9486. http://dx.doi.org/10.1073/pnas.1307473110.
3. **Plante K, Wang E, Partidos CD, Weger J, Gorchakov R, Tsetsarkin K, Borland EM, Powers AM, Seymour R, Stinchcomb DT, Osorio JE, Frolov I, Weaver SC.** 2011. Novel chikungunya vaccine candidate with an IRES-based attenuation and host range alteration mechanism. PLoS Pathog. **7:**e1002142. http://dx.doi.org/10.1371/journal.ppat.1002142.
4. **Guerbois M, Volkova E, Forrester NL, Rossi SL, Frolov I, Weaver SC.** 2013. IRES-driven expression of the capsid protein of the Venezuelan equine encephalitis virus TC-83 vaccine strain increases its attenuation and safety. PLoS Negl. Trop. Dis. **7:**e2197. http://dx.doi.org/10.1371/journal.pntd.0002197.
5. **Rossi SL, Guerbois M, Gorchakov R, Plante KS, Forrester NL, Weaver SC.** 2013. IRES-based Venezuelan equine encephalitis vaccine candidate elicits protective immunity in mice. Virology **437:**81–88. http://dx.doi.org/10.1016/j.virol.2012.11.013.
6. **Volkova E, Frolova E, Darwin JR, Forrester NL, Weaver SC, Frolov I.** 2008. IRES-dependent replication of Venezuelan equine encephalitis virus makes it highly attenuated and incapable of replicating in mosquito cells. Virology **377:**160–169. http://dx.doi.org/10.1016/j.virol.2008.04.020.
7. **Borden EC, Sen GC, Uze G, Silverman RH, Ransohoff RM, Foster GR, Stark GR.** 2007. Interferons at age 50: past, current and future impact on biomedicine. Nat. Rev. Drug Discov. **6:**975–990. http://dx.doi.org/10.1038/nrd2422.
8. **Pestka S, Krause CD, Walter MR.** 2004. Interferons, interferon-like cytokines, and their receptors. Immunol. Rev. **202:**8–32. http://dx.doi.org/10.1111/j.0105-2896.2004.00204.x.
9. **Colonna M, Krug A, Cella M.** 2002. Interferon-producing cells: on the front line in immune responses against pathogens. Curr. Opin. Immunol. **14:**373–379. http://dx.doi.org/10.1016/S0952-7915(02)00349-7.
10. **Schoggins JW, Wilson SJ, Panis M, Murphy MY, Jones CT, Bieniasz P, Rice CM.** 2011. A diverse range of gene products are effectors of the type I interferon antiviral response. Nature **472:**481–485. http://dx.doi.org/10.1038/nature09907.
11. **Gonzalez-Navajas JM, Lee J, David M, Raz E.** 2012. Immunomodulatory functions of type I interferons. Nat. Rev. Immunol. **12:**125–135. http://dx.doi.org/10.1038/nri3133.
12. **Rizza P, Capone I, Moretti F, Proietti E, Belardelli F.** 2011. IFN-alpha as a vaccine adjuvant: recent insights into the mechanisms and perspectives for its clinical use. Expert Rev. Vaccines **10:**487–498. http://dx.doi.org/10.1586/erv.11.9.
13. **Day SL, Ramshaw IA, Ramsay AJ, Ranasinghe C.** 2008. Differential effects of the type I interferons alpha4, beta, and epsilon on antiviral activity and vaccine efficacy. J. Immunol. **180:**7158–7166.
14. **Faul EJ, Wanjalla CN, McGettigan JP, Schnell MJ.** 2008. Interferon-beta expressed by a rabies virus-based HIV-1 vaccine vector serves as a molecular adjuvant and decreases pathogenicity. Virology **382:**226–238. http://dx.doi.org/10.1016/j.virol.2008.09.019.
15. **Kirn DH, Wang Y, Le Boeuf F, Bell J, Thorne SH.** 2007. Targeting of interferon-beta to produce a specific, multi-mechanistic oncolytic vaccinia virus. PLoS Med. **4:**e353. http://dx.doi.org/10.1371/journal.pmed.0040353.
16. **Odaka M, Sterman DH, Wiewrodt R, Zhang Y, Kiefer M, Amin KM, Gao GP, Wilson JM, Barsoum J, Kaiser LR, Albelda SM.** 2001. Eradication of intraperitoneal and distant tumor by adenovirus-mediated interferon-beta gene therapy is attributable to induction of systemic immunity. Cancer Res. **61:**6201–6212.
17. **Willmon CL, Saloura V, Fridlender ZG, Wongthida P, Diaz RM, Thompson J, Kottke T, Federspiel M, Barber G, Albelda SM, Vile RG.** 2009. Expression of IFN-beta enhances both efficacy and safety of oncolytic vesicular stomatitis virus for therapy of mesothelioma. Cancer Res. **69:**7713–7720. http://dx.doi.org/10.1158/0008-5472.CAN-09-1013.
18. **Mullbacher A, Lobigs M, Lee E.** 2003. Immunobiology of mosquito-borne encephalitic flaviviruses. Adv. Virus Res. **60:**87–120. http://dx.doi.org/10.1016/S0065-3527(03)60003-5.
19. **Lobigs M, Diamond MS.** 2012. Feasibility of cross-protective vaccination against flaviviruses of the Japanese encephalitis serocomplex. Expert Rev. Vaccines **11:**177–187. http://dx.doi.org/10.1586/erv.11.180.
20. **Müller U, Steinhoff U, Reis LF, Hemmi S, Pavlovic J, Zinkernagel RM, Aguet M.** 1994. Functional role of type I and type II interferons in antiviral defense. Science **264:**1918–1921. http://dx.doi.org/10.1126/science.8009221.
21. **Prochazka M, Gaskins HR, Shultz LD, Leiter EH.** 1992. The nonobese diabetic scid mouse: model for spontaneous thymomagenesis associated with immunodeficiency. Proc. Natl. Acad. Sci. U. S. A. **89:**3290–3294. http://dx.doi.org/10.1073/pnas.89.8.3290.
22. **Lee E, Lobigs M.** 2000. Substitutions at the putative receptor-binding site of an encephalitic flavivirus alter virulence and host cell tropism and reveal a role for glycosaminoglycans in entry. J. Virol. **74:**8867–8875. http://dx.doi.org/10.1128/JVI.74.19.8867-8875.2000.
23. **Licon Luna RM, Lee E, Müllbacher A, Blanden RV, Langman R, Lobigs M.** 2002. Lack of both Fas ligand and perforin protects from flavivirus-mediated encephalitis in mice. J. Virol. **76:**3202–3211. http://dx.doi.org/10.1128/JVI.76.7.3202-3211.2002.
24. **Bochkov YA, Palmenberg AC.** 2006. Translational efficiency of EMCV IRES in bicistronic vectors is dependent upon IRES sequence and gene location. Biotechniques **41:**283–284. http://dx.doi.org/10.2144/000112243.
25. **Lobigs M, Lee E, Ng ML, Pavy M, Lobigs P.** 2010. A flavivirus signal peptide balances the catalytic activity of two proteases and thereby facilitates virus morphogenesis. Virology **401:**80–89. http://dx.doi.org/10.1016/j.virol.2010.02.008.
26. **Sutcliffe EL, Parish IA, He YQ, Juelich T, Tierney ML, Rangasamy D, Milburn PJ, Parish CR, Tremethick DJ, Rao S.** 2009. Dynamic histone variant exchange accompanies gene induction in T cells. Mol. Cell. Biol. **29:**1972–1986. http://dx.doi.org/10.1128/MCB.01590-08.
27. **Lee E, Hall RA, Lobigs M.** 2004. Common E protein determinants for attenuation of glycosaminoglycan-binding variants of Japanese encephalitis and West Nile viruses. J. Virol. **78:**8271–8280. http://dx.doi.org/10.1128/JVI.78.15.8271-8280.2004.

28. **Colombage G, Hall R, Pavy M, Lobigs M.** 1998. DNA-based and alphavirus-vectored immunisation with prM and E proteins elicits long-lived and protective immunity against the flavivirus, Murray Valley encephalitis virus. Virology **250:**151–163. http://dx.doi.org/10.1006/viro.1998.9357.
29. **Lobigs M, Pavy M, Hall RA, Lobigs P, Cooper P, Komiya T, Toriniwa H, Petrovsky N.** 2010. An inactivated Vero cell-grown Japanese encephalitis vaccine formulated with Advax, a novel inulin-based adjuvant, induces protective neutralizing antibody against homologous and heterologous flaviviruses. J. Gen. Virol. **91:**1407–1417. http://dx.doi.org/10.1099/vir.0.019190-0.
30. **Flohr F, Schneider-Schaulies S, Haller O, Kochs G.** 1999. The central interactive region of human MxA GTPase is involved in GTPase activation and interaction with viral target structures. FEBS Lett. **463:**24–28. http://dx.doi.org/10.1016/S0014-5793(99)01598-7.
31. **Clark DC, Lobigs M, Lee E, Howard MJ, Clark K, Blitvich BJ, Hall RA.** 2007. In situ reactions of monoclonal antibodies with a viable mutant of Murray Valley encephalitis virus reveal an absence of dimeric NS1 protein. J. Gen. Virol. **88:**1175–1183. http://dx.doi.org/10.1099/vir.0.82609-0.
32. **Larena M, Regner M, Lee E, Lobigs M.** 2011. Pivotal role of antibody and subsidiary contribution of CD8+ T cells to recovery from infection in a murine model of Japanese encephalitis. J. Virol. **85:**5446–5455. http://dx.doi.org/10.1128/JVI.02611-10.
33. **Desmyter J, Melnick JL, Rawls WE.** 1968. Defectiveness of interferon production and of rubella virus interference in a line of African green monkey kidney cells (Vero). J. Virol. **2:**955–961.
34. **Lobigs M, Marshall ID, Weir RC, Dalgarno L.** 1988. Murray Valley encephalitis virus field strains from Australia and Papua New Guinea: studies on the sequence of the major envelope protein gene and virulence for mice. Virology **165:**245–255. http://dx.doi.org/10.1016/0042-6822(88)90678-2.
35. **Lobigs M, Mullbacher A, Wang Y, Pavy M, Lee E.** 2003. Role of type I and type II interferon responses in recovery from infection with an encephalitic flavivirus. J. Gen. Virol. **84:**567–572. http://dx.doi.org/10.1099/vir.0.18654-0.
36. **Hoenen A, Liu W, Kochs G, Khromykh AA, Mackenzie JM.** 2007. West Nile virus-induced cytoplasmic membrane structures provide partial protection against the interferon-induced antiviral MxA protein. J. Gen. Virol. **88:**3013–3017. http://dx.doi.org/10.1099/vir.0.83125-0.
37. **Roers A, Hochkeppel HK, Horisberger MA, Hovanessian A, Haller O.** 1994. MxA gene expression after live virus vaccination: a sensitive marker for endogenous type I interferon. J. Infect. Dis. **169:**807–813. http://dx.doi.org/10.1093/infdis/169.4.807.
38. **Haller O, Stertz S, Kochs G.** 2007. The Mx GTPase family of interferon-induced antiviral proteins. Microbes Infect. **9:**1636–1643. http://dx.doi.org/10.1016/j.micinf.2007.09.010.
39. **Horisberger MA, De Staritzky K.** 1989. Expression and stability of the Mx protein in different tissues of mice, in response to interferon inducers or to influenza virus infection. J. Interferon Res. **9:**583–590. http://dx.doi.org/10.1089/jir.1989.9.583.
40. **Ronni T, Melen K, Malygin A, Julkunen I.** 1993. Control of IFN-inducible MxA gene expression in human cells. J. Immunol. **150:**1715–1726.
41. **Larena M, Prow NA, Hall RA, Petrovsky N, Lobigs M.** 2013. JE-ADVAX vaccine protection against Japanese encephalitis virus mediated by memory B cells in the absence of CD8(+) T cells and preexposure neutralizing antibody. J. Virol. **87:**4395–4402. http://dx.doi.org/10.1128/JVI.03144-12.
42. **Petrovsky N, Larena M, Siddharthan V, Prow NA, Hall RA, Lobigs M, Morrey J.** 2013. An inactivated cell culture Japanese encephalitis vaccine (JE-ADVAX) formulated with delta inulin adjuvant provides robust heterologous protection against West Nile encephalitis via cross-protective memory B cells and neutralizing antibody. J. Virol. **87:**10324–10333. http://dx.doi.org/10.1128/JVI.00480-13.
43. **Stocks CE, Lobigs M.** 1995. Posttranslational signal peptidase cleavage of the flavivirus C-prM junction, in vitro. J. Virol. **69:**8123–8126.
44. **Stocks CE, Lobigs M.** 1998. Signal peptidase cleavage at the flavivirus C-prM junction: dependence on the viral NS2B-3 protease for efficient processing requires determinants in C, the signal peptide, and prM. J. Virol. **72:**2141–2149.
45. **Lobigs M, Lee E.** 2004. Inefficient signalase cleavage promotes efficient nucleocapsid incorporation into budding flavivirus membranes. J. Virol. **78:**178–186. http://dx.doi.org/10.1128/JVI.78.1.178-186.2004.
46. **Lobigs M, Mullbacher A, Lee E.** 2004. Evidence that a mechanism for efficient flavivirus budding upregulates MHC class I. Immunol. Cell Biol. **82:**184–188. http://dx.doi.org/10.1046/j.0818-9641.2004.01218.x.
47. **Lobigs M, Mullbacher A, Regner M.** 2003. MHC class I up-regulation by flaviviruses: immune interaction with unknown advantage to host or pathogen. Immunol. Cell Biol. **81:**217–223. http://dx.doi.org/10.1046/j.1440-1711.2003.01161.x.
48. **Momburg F, Mullbacher A, Lobigs M.** 2001. Modulation of transporter associated with antigen processing (TAP)-mediated peptide import into the endoplasmic reticulum by flavivirus infection. J. Virol. **75:**5663–5671. http://dx.doi.org/10.1128/JVI.75.12.5663-5671.2001.
49. **Van Gessel Y, Klade CS, Putnak R, Formica A, Krasaesub S, Spruth M, Cena B, Tungtaeng A, Gettayacamin M, Dewasthaly S.** 2011. Correlation of protection against Japanese encephalitis virus and JE vaccine (IXIARO((R))) induced neutralizing antibody titers. Vaccine **29:**5925–5931. http://dx.doi.org/10.1016/j.vaccine.2011.06.062.
50. **Kalvakolanu DV.** 2003. Alternate interferon signaling pathways. Pharmacol. Ther. **100:**1–29. http://dx.doi.org/10.1016/S0163-7258(03)00070-6.
51. **Samuel CE, Farris DA.** 1977. Mechanism of interferon action. Species specificity of interferon and of the interferon-mediated inhibitor of translation from mouse, monkey, and human cells. Virology **77:**556–565.
52. **Pierson TC, Diamond MS, Ahmed AA, Valentine LE, Davis CW, Samuel MA, Hanna SL, Puffer BA, Doms RW.** 2005. An infectious West Nile virus that expresses a GFP reporter gene. Virology **334:**28–40. http://dx.doi.org/10.1016/j.virol.2005.01.021.
53. **Yun SI, Choi YJ, Yu XF, Song JY, Shin YH, Ju YR, Kim SY, Lee YM.** 2007. Engineering the Japanese encephalitis virus RNA genome for the expression of foreign genes of various sizes: implications for packaging capacity and RNA replication efficiency. J. Neurovirol. **13:**522–535. http://dx.doi.org/10.1080/13550280701684651.
54. **Deas TS, Binduga-Gajewska I, Tilgner M, Ren P, Stein DA, Moulton HM, Iversen PL, Kauffman EB, Kramer LD, Shi PY.** 2005. Inhibition of flavivirus infections by antisense oligomers specifically suppressing viral translation and RNA replication. J. Virol. **79:**4599–4609. http://dx.doi.org/10.1128/JVI.79.8.4599-4609.2005.
55. **Shustov AV, Mason PW, Frolov I.** 2007. Production of pseudoinfectious yellow fever virus with a two-component genome. J. Virol. **81:**11737-11748. http://dx.doi.org/10.1128/JVI.01112-07.
56. **Zou G, Xu HY, Qing M, Wang QY, Shi PY.** 2011. Development and characterization of a stable luciferase dengue virus for high-throughput screening. Antiviral Res. **91:**11–19. http://dx.doi.org/10.1016/j.antiviral.2011.05.001.
57. **Lavoie TB, Kalie E, Crisafulli-Cabatu S, Abramovich R, DiGioia G, Moolchan K, Pestka S, Schreiber G.** 2011. Binding and activity of all human alpha interferon subtypes. Cytokine **56:**282–289. http://dx.doi.org/10.1016/j.cyto.2011.07.019.
58. **Gibbert K, Dittmer U.** 2011. Distinct antiviral activities of IFN-alpha subtypes. Immunotherapy **3:**813–816. http://dx.doi.org/10.2217/imt.11.74.
59. **James CM, Abdad MY, Mansfield JP, Jacobsen HK, Vind AR, Stumbles PA, Bartlett EJ.** 2007. Differential activities of alpha/beta IFN subtypes against influenza virus in vivo and enhancement of specific immune responses in DNA vaccinated mice expressing haemagglutinin and nucleoprotein. Vaccine **25:**1856–1867. http://dx.doi.org/10.1016/j.vaccine.2006.10.038.
60. **Dalgarno L, Trent DW, Strauss JH, Rice CM.** 1986. Partial nucleotide sequence of the Murray Valley encephalitis virus genome. J. Mol. Biol. **187:**309–323. http://dx.doi.org/10.1016/0022-2836(86)90435-3.